

Interpreting palaeofire evidence from fluvial sediments: a case study from Santa Rosa Island, California, with implications for the Younger Dryas Impact Hypothesis

ANDREW C. SCOTT,^{1*} MARK HARDIMAN,² NICHOLAS PINTER,³ R. SCOTT ANDERSON,⁴ TYRONE L. DAULTON,^{5,6} ANA EJARQUE,^{7,8} PAUL FINCH⁹ and ALICE CARTER-CHAMPION¹⁰

¹Department of Earth Sciences, Royal Holloway University of London, Egham, Surrey TW20 0EX, UK

²Department of Geography, University of Portsmouth, Portsmouth PO1 3HE, UK

³Department of Earth and Planetary Sciences, University of California, Davis, CA 95616, USA

⁴School of Earth Sciences and Environmental Sustainability, Northern Arizona University, Flagstaff, AZ 86011, USA

⁵Washington University in St. Louis, Department of Physics and Laboratory for Space Sciences, St. Louis, MO 63130, USA

⁶Institute for Materials Science and Engineering, Washington University in St. Louis, St. Louis, MO 63130, USA

⁷CNRS, UMR 6042, GEOLAB, Clermont-Ferrand, France

⁸Clermont Université, Université Blaise Pascal, GEOLAB, BP 10448, Clermont-Ferrand, France

⁹School of Biological Sciences, Royal Holloway University of London, Egham, Surrey TW20 0EX, UK

¹⁰Department of Geography, Royal Holloway University of London, Egham, Surrey TW20 0EX, UK

Received 25 June 2015; Revised 28 September 2016; Accepted 10 October 2016

ABSTRACT: Fluvial sequences from the late Pleistocene to the Holocene are exposed in Arlington Canyon, Santa Rosa Island, Northern Channel Islands, California, USA, including one outcrop that features centrally in the controversial hypothesis of an extra-terrestrial impact at the onset of the Younger Dryas. The fluvial sequence in Arlington Canyon contains a significant quantity and range of organic material, much of which has been charred. The purpose of this study was to systematically describe the key outcrop of the Arlington sequence, provide new radiocarbon age control and analyse organic material in the Arlington sediments within a rigorous palaeobotanical and palaeo-charcoal context. These analyses provide a test of previous claims for catastrophic impact-induced fire in Arlington Canyon. Carbonaceous spherular materials were identified as predominantly fungal sclerotia; ‘carbon elongates’ are predominantly arthropod coprolites, including termite frass. ‘Glassy carbon’ formed from the precipitation of tars during charcoalification. None of these materials indicate high-temperature formation or combustion. Charcoal and other materials in Arlington Canyon document widespread and frequent fires both before and after the onset of the Younger Dryas, recording predominantly low-temperature surface fires. In summary, we find no evidence in Arlington Canyon for an extra-terrestrial impact or catastrophic impact-induced fire. Copyright © 2016 John Wiley & Sons, Ltd.

KEYWORDS: charcoal; extra-terrestrial impact; fluvial sedimentology; stratigraphy; Younger Dryas Impact Hypothesis.

Introduction

Quaternary fluvial records provide information on terrestrial palaeoclimate (e.g. Pigati *et al.*, 2014), neotectonics (e.g. Pinter and Keller, 1995), archaeological context (Mishra *et al.*, 2007) and a wide variety of other areas (see Bridgland and Westaway, 2014). These sediments offer unique challenges, and failure to consider these may hamper or, worse, lead to erroneous palaeoenvironmental interpretations.

The Younger Dryas Stadial, which corresponds to Greenland Stadal-1 (GS-1; ~12.9–11.7 ka BP; Rasmussen *et al.*, 2006) has been well described and has been recognized in proxy records from California (e.g. Hendy *et al.*, 2002). The ‘Younger Dryas Impact Hypothesis’ (YDIH) is the relatively new suggestion (Firestone *et al.*, 2007) that global events approximately 12.9 ka BP – including climatic cooling, extinction of North American megafauna, demise of the Clovis archaeological culture and other changes worldwide – resulted from the impact of a 5-km-diameter comet into the southern margin of the Laurentide ice sheet. The YDIH is controversial and has been heavily contested (e.g. Pinter and Ishman, 2008; Pinter *et al.*, 2011; Boslough *et al.*, 2013; van Hoesel *et al.*, 2014; Holliday *et al.*, 2014; Meltzer *et al.*, 2014; Daulton *et al.*,

2016). Although many sites globally have been put forward as containing evidence for the YDIH (e.g. LeCompte *et al.*, 2012; Bunch *et al.*, 2012; Wittke *et al.*, 2013; Petaev *et al.*, 2013) one key sedimentary section from Arlington Canyon, Santa Rosa Island, in the Northern Channel Islands of California (Fig. 1) has played a particularly important role in the ongoing development of the YDIH (AC003 in Kennett *et al.*, 2008 *et seq*; site III in this study). Several key papers have focused on this locality with the interpretation of ‘intense biomass burning’ and associated rapid landscape change (Kennett *et al.*, 2008), the presence of nanodiamonds (Kennett *et al.*, 2009a) and shock-synthesized hexagonal diamonds (Kennett *et al.*, 2009b). More recently, dating evidence from the site was a key component used in a Bayesian chronological analysis which found a synchronous age for the start of the Younger Dryas boundary or ‘impact’ layer (Kennett *et al.*, 2015).

The purpose of this study was to systematically sample locality AC003 (Kennett *et al.*, 2008 *et seq*; site III in this study) in Arlington Canyon for its evidence of palaeofire and relate this single site stratigraphy to other multiple sites along the canyon that we also investigated for fire history (see Pinter *et al.*, 2011; Hardiman *et al.*, 2016). We demonstrate that evidence in Arlington Canyon is inconsistent with the catastrophic extraterrestrial impact and the associated local manifestations that have been proposed. More broadly,

*Correspondence: A. C. Scott, as above.

E-mail: a.scott@rhul.ac.uk

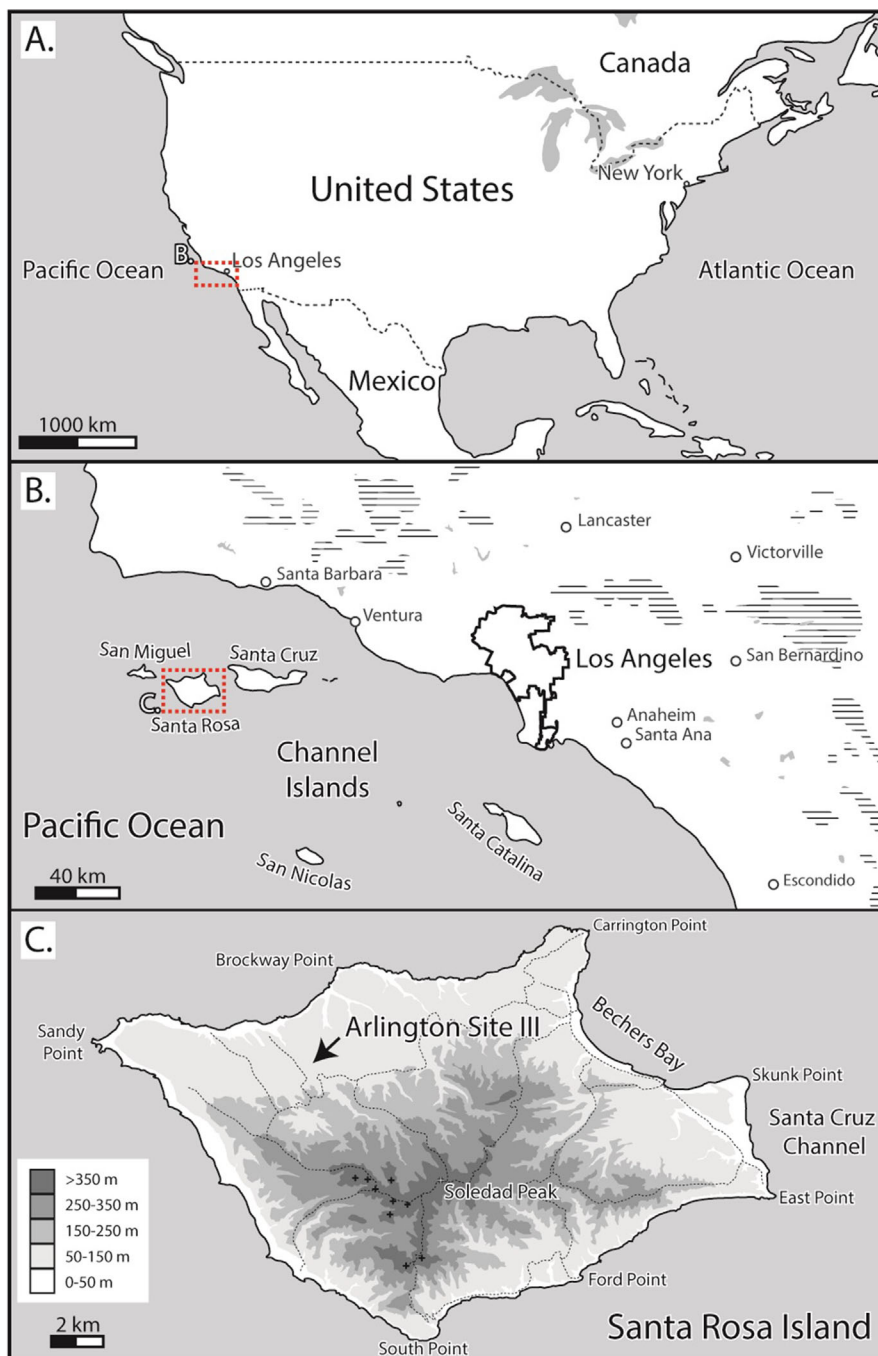


Figure 1. Map of Santa Rosa showing location of Section III (AC003 of Kennett *et al.*, 2008).

the widely divergent interpretations of events preserved in Arlington Canyon illustrate general challenges in using palaeobotanical and charcoal records from fluvial sequences. We present recommendations and protocols for analysis of Quaternary fluvial deposits, particularly for the collection of macro-charcoal (defined here as having sizes $>125\ \mu\text{m}$) and interpretation of palaeofire from these more complex sedimentary sequences.

Material and methods

Arlington Canyon is one of a series of N–S drainages along the northern flank of Santa Rosa Island, carrying discharge from the island's interior northward to the coast (Fig 1). Santa Rosa Island has been slowly uplifting through the Quaternary (Pinter *et al.*, 2001), resulting in rugged topography and streams within deeply incised canyons (Schumann *et al.*, 2016). At the base of Arlington and selected neighbouring canyons, one aggradational terrace level forms a

morphological bench up to $\sim 25\ \text{m}$ above the modern stream. This terrace sedimentary fill consists of fluvial and localized colluvial deposits that aggraded from the canyon base during the latest Pleistocene until the mid-to late Holocene (Pinter *et al.*, 2001; Schumann *et al.*, 2014). This was followed by a cessation of deposition and reinitiation of incision that cut base level to the bottom of the canyon and exposed the Pleistocene to Holocene fill deposits in a narrow 'slot canyon' through the terrace (Schumann *et al.*, 2016). The terrace fill sequence consists of several fluvial cut-and-fill packages, consisting of channel and floodplain deposits that pinch out laterally or grade into colluvial deposits at their margins. Distinguishable stratigraphic units can be traced laterally over distances of metres to tens of metres, but these fluvial units change in texture and character both vertically and horizontally. Sandy point bars and silt-dominated overbank deposits are punctuated by conglomeratic channel fills. Distinguishable depositional units range in thickness from $<1\ \text{m}$ to more than $10\ \text{m}$. Between cut-and-fill packages,

several depositional hiatuses and erosional unconformities are marked by weakly developed palaeosols, characterized by darker colour (Pinter *et al.*, 2011; Schumann *et al.*, 2014), enriched clay content and weak soil structure developed on these undulating palaeo-topographic surfaces.

Our Locality I (see Scott *et al.*, 2010 supplementary data) is an exposure more than 10m high and 100m long (33° 59'19.28"N, 120°9'32.03"W [WGS84]). Our Localities II and III are located just 110 and 190m north, respectively, of Locality I, but the lateral variability in the fluvial architecture makes it impossible to correlate sections at the scale of individual units. Locality III is a 4-m-high exposure on the western side of the canyon (33° 59' 25.73"N, 120° 9' 32.22"W [WGS84]) (see Supplementary Materials, Fig. S1). Wittke *et al.* (2013) claim that 'coordinates, photographs, stratigraphic descriptions, and radiocarbon ages presented in their papers (e.g. Scott *et al.*, 2010 and Pinter *et al.*, 2011) conclusively demonstrate that none of their samples collected were taken from the same stratigraphic section studied by

Kennett *et al.* (2008).' On the contrary, our Locality III is identical to their locality AC003 (see Supplementary Materials, Fig. S2). Furthermore, material from AC003 was sent to the senior author in March 2007 by G. James West (via John Johnson) with a request to report on the charcoal. Lithological logs of other Arlington sections and radiocarbon data are given in Hardiman *et al.* (2016).

Sampling procedures

The large changes in depositional facies over short distances within the Arlington Canyon fluvial sequence, combined with high vertical-relief and cut-and-fill sedimentary packages require extensive detail in the stratigraphic descriptions (Fig. 2) and a large number of dated samples to correlate packages of sedimentary aggradation through the full sequence. Our sampling goals included: (i) to collect organic material in the sediments, with particular interest in charcoalified plants (macrocharcoal, >125 µm), and (ii) to obtain material for

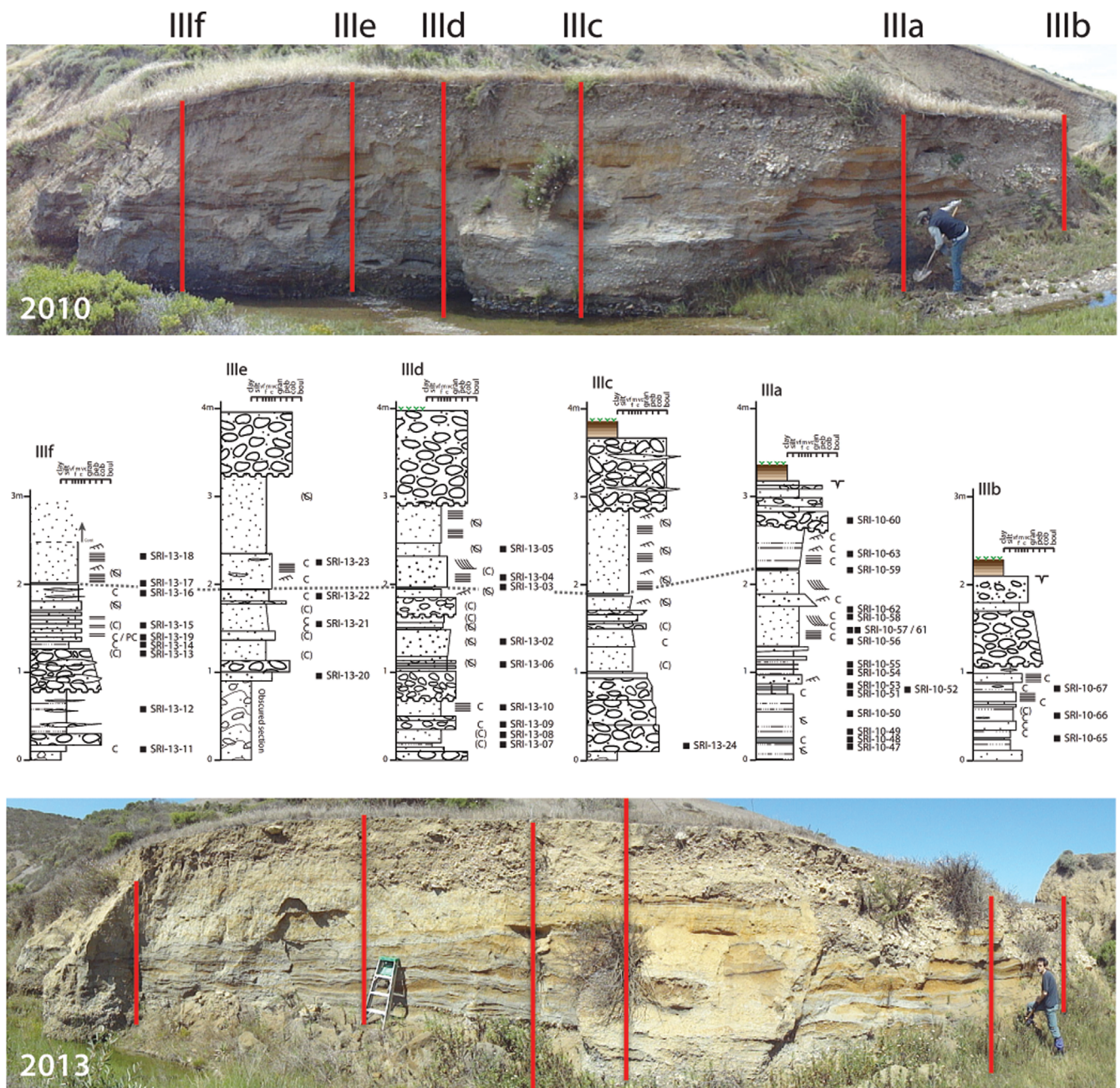


Figure 2. Detailed lithological logs (for key see Fig S1) of site III, Arlington Canyon, showing the site in 2010 (above) and 2013 (below).

radiocarbon dating. Thus, we sampled every horizon with visible charcoal. At some intervals where continuous sampling was necessary, we used a core box that could be hammered into the section and removed for later sub-sampling. All samples were photographed *in situ* before removal.

Sample processing and radiocarbon dating

To separate charcoal or macroscopic plant material from bulk sediment, we first removed any large rock clasts. Sediment was then soaked in warm water for disaggregation; if needed we used 10% hydrogen peroxide (Rhodes, 1998). It should be noted that the charcoal in such water baths generally does not float off, as suggested by Firestone *et al.* (2007). The samples were then wet sieved to produce residues of below 62 μm , below 125 μm and above 125 μm . Charcoal was picked from the >125- μm residues. We note that in all samples, charcoal pieces are liable to fragment, so counts of number of fragments are not meaningful, particularly in fluvial sediments. Some of the charcoal residues were cleaned by dissolving the sediment in 40% HF (see Scott, 2010).

Particularly for fluvial deposits, a pervasive issue for radiocarbon dating is the potential for 'old wood' charcoal dates (Schiffer, 1986; Gavin, 2001; Bird, 2013). Because charcoal is chemically inert and mechanically robust, it can sometimes survive erosion from a preexisting deposit, transport through the fluvial system and redeposition. To minimize the danger of dating secondary, re-deposited charcoal, we identified organic material before submission for radiocarbon analysis and selected only fragile but well-preserved charred plant parts, rather than more robust charcoal fragments. Picked samples of charcoaled wood, seeds, carbonaceous spherules and coprolites were sent for radiocarbon dating by two different laboratories: the Keck Carbon Cycle AMS Laboratory at University of California (UC) Irvine and the Oxford Radiocarbon Accelerator Unit, RLAHA, University of Oxford (see Hardiman *et al.*, 2016).

There are several methods to separate charcoaled plant material from disaggregated sediment samples (see Scott, 2010). Samples picked from sediments were studied by light microscopy or mounted on aluminium stubs for scanning electron microscopy. Some charcoal was embedded into resin blocks and polished for examination under oil reflective microscopy. We attempted to use the protocol outlined in Firestone *et al.* (2007) and Kennett *et al.* (2008, 2009b) for specimen isolation, but following these we were not successful. We found that none of the charcoal separation techniques cited in Firestone *et al.* (2007) worked for the Arlington samples, so it is uncertain how these were collected, processed or picked. Sampling protocols provided in 'Separation of YD Event Markers (8/10/2007)', a guide provided by one of its authors (Allen West, GeoScience Consulting), will break up charcoal fragments into a large number of smaller fragments.

Microscopy of palaeobotanical samples

Samples were identified under water by reflected light under a low-power binocular microscope. Some samples were picked using dark-field lighting (see Glasspool and Scott, 2013) that facilitated the separation of charred and uncharred plant fragments. Some specimens were gold-coated using a Poloron sputter coater. Uncoated specimens were studied using a Hitachi S3000N variable pressure scanning electron microscope under low vacuum and in backscatter electron mode. Coated samples were studied using secondary electron mode. Specimens were also gold coated and examined using a Philips environmental scanning electron microscope.

Uncharred and charred carbonaceous 'spherules', 'elongates' and wood charcoals were embedded in polyester resin, cut and polished. Reflectance was measured using a Leica DM2500 microscope linked to an MSP200 photometer reflectance system. The specimens were measured under oil of refractive index 1.518, using light filtered to 546 nm. Mean random reflectance (R_o %) was measured, and temperature conversion was achieved by comparison with wood and fungus charcoal experimental charcoalification curves. Full charcoal reflectance methodology and background are presented in Scott and Glasspool (2005, 2007), McParland *et al.* (2009) and Scott (2010).

Organic geochemistry (analytical pyrolysis)

Analytical pyrolysis was carried out using an SGE Pyrojector pressurized with helium at 15 psi and fitted to an HP5890 Series II gas chromatograph interfaced to an HP5972 MSD mass spectrometer at Royal Holloway University of London. Samples (~1 mg) were loaded into and introduced with a P-3 pelletizer, and pyrolysis was carried out at 650 °C. Pyrolysate was transferred to the chromatography column with a constant flow of helium of 0.7 cm³ min⁻¹ into the gas chromatograph inlet kept at 280 °C. The column (J&W DB5, 30 m × 0.25 mm × 0.25 μm film thickness) was initially at 50 °C for 2 min, then heated at 7.5 °C min⁻¹ to a final temperature of 330 °C. Splitless injection was applied with a delay time of 1.5 min, and the gas chromatograph – mass spectrometer interface temperature was set at 300 °C.

Sedimentological, stratigraphical and biological description

Along much of the Arlington Canyon study area, the basal 1–2 m of Quaternary fill consists of horizontal to sub-horizontally bedded silt-dominated strata, with dispersed sand-size grains. We sampled and measured as low in the section as possible, sometimes hand-excavating several decimetres below groundwater level. Because the basal sediments were wet in outcrop, they gave the impression of being darker in colour and, seemingly, more organic-rich (Kennett *et al.*, 2008, 2009b). This was not the case; the samples lightened to a grey-brown colour upon drying (Fig. 2; Supplementary Materials, Fig. S3).

Within these fine-grained basal facies are isolated sand- and gravel-rich laminae that occur as lenses, bar forms, and thin channels (Figs 2 and S3). This coarser clastic fraction includes small rounded granules and pebbles and a few, isolated more angular and larger rock fragments. Some of the horizons contain charcoal, but the charred fragments were not uniformly distributed within them. Conglomeratic units occurred as lenses or as distinct channel fills. The base of Section IIIc, for example, comprises a >1-m-thick gravel layer. Less than 8 m to the north, this horizon has thinned and is no longer present (Log IIIa). Log IIIb is located identically to the section described by Kennett *et al.* (2008, 2009b), and the photograph showing the position of their recorded section is shown in Wittke *et al.* (2013, supplementary information) and here in Fig. S2.

Overlying the basal, predominantly fine-grained deposits in Arlington Canyon is a sand-dominated package, consisting predominately of laminated and cross-bedded sands. Charcoal and charred plant fragments are widespread, ranging in size up to >1 cm in diameter (see Fig. S4); some horizons also contain un-charred and partially charred plant material. Within the coarse sands, there are abundant coarser granule lenses and isolated pebbles (Fig. S5). At Locality III at the ~2-m level, there is a thin clay-rich band, dark but not

organic-rich, that is clearly identifiable on the log and photos of Kennett *et al.* (2008, 2009b) and Wittke *et al.* (2013) (Fig. 2). The next metre higher in the section at Locality III is predominantly fine sand with some cross beds, scattered charcoal fragments (Fig. 2) and some coarse sand that often fills small channels (Fig. 2). This unit is crosscut by an erosional ravinement surface that is widespread in Arlington

Canyon, locally high in relief and down-cutting through the underlying units by >10 m in some locations.

Charcoal distribution and identification

Charcoal (Figs 3 and 4; Supplementary Material, Fig. S6) in the Arlington Canyon sequence, especially wood charcoal, is concentrated in the basal ~3 m of the sections (Table 1).

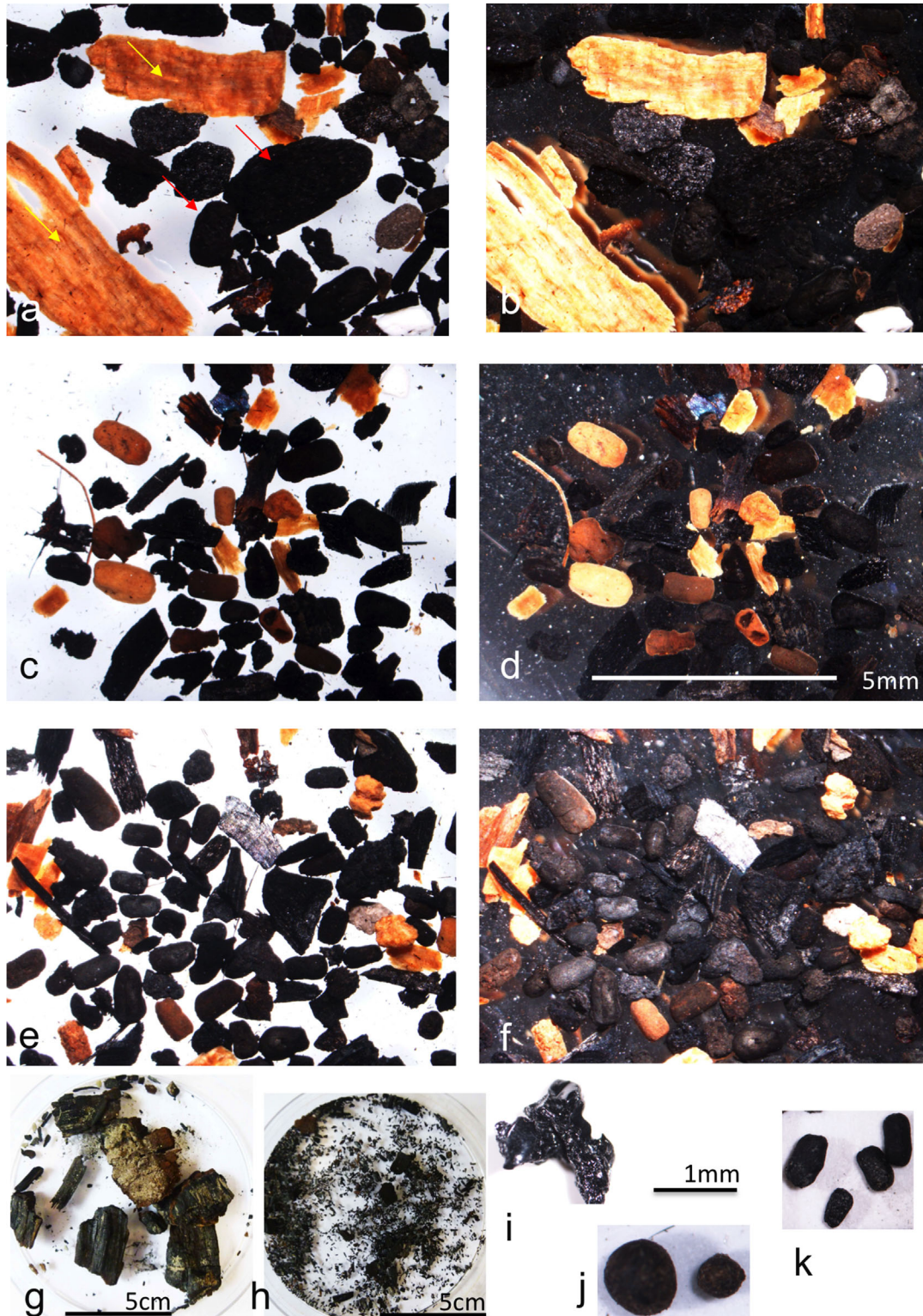


Figure 3. Organic fractions from sieved samples, Site III, Arlington Canyon. Images (a,c,e) are reflected light under water; images (b,d,f) are dark field images of the same samples highlighting charred and uncharred plant material. (a,b) Sample 10-56 Section IIIa mid section. The image shows large uncharred wood fragments (brown) (yellow arrows) with wood charcoal (black) (red arrows) and coprolites. (c,d) Sample 10-56 Section IIIa mid section. (e,f) Sample 10-56 Section IIIa mid section. (g) Large charcoal fragments, sample SRI-13-19, Section IIIf below mid section. (h) Specimen of wood charcoal shown in (g) and put into water showing fragmentation. (i) Glassy carbon, sample SRI-10-56, Section IIIa. (j) Carbonaceous spherules, sample SRI-10-56, Section IIIj. (k) Carbon elongates (coprolites). Sample SRI-10-56, Section IIIa.

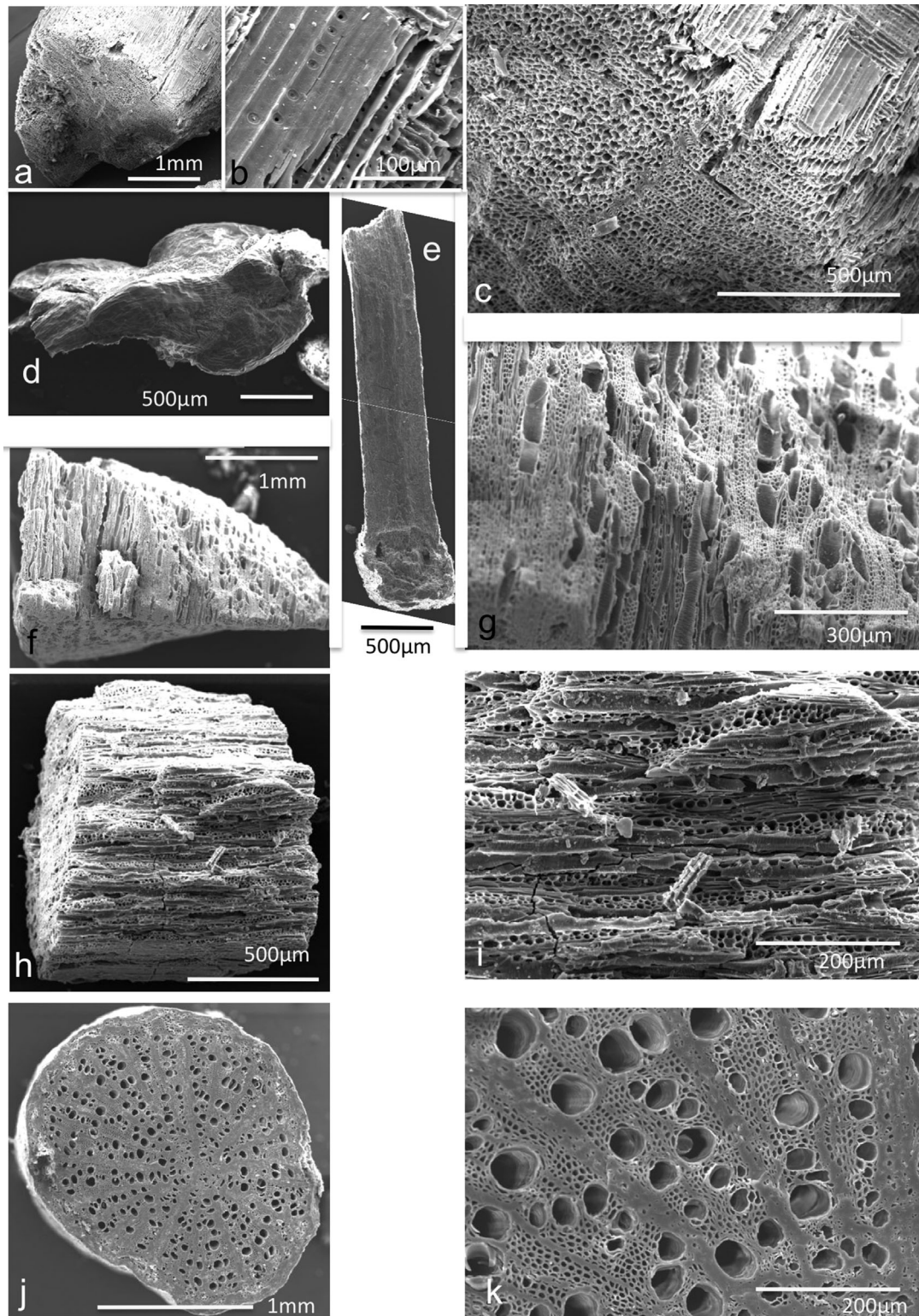


Figure 4. Charcoal from sediments from Site III, Arlington Canyon. (a) Scanning electron micrograph of conifer secondary wood, SRI-10-65, Section IIIc. (b) Detail of image (a) showing rays and ray pits. (c) Detail of image (a) showing growth ring. (d) Conifer leafy shoot, cf *Cupressus* sp., SRI-13 = 11, Section IIIc. (e) Conifer needle, *Pinus* sp., SRI-13-21. (f) Angiosperm secondary wood, SRI-13 core IIIID, 37 cm from base. (g) Detail of image (f) showing vessels. (h) Angiosperm secondary wood, SRI-13-21. (i) Detail of image (h) showing multiseriate rays. (j) Small angiosperm axis, SRI-13 core IIIID, 37 cm from base. (k) Detail of image (j) showing vessels.

Charcoal becomes less common higher in the sequence. Charcoal occurs as thin discontinuous layers, lenses and as scattered fragments (Fig. S4). In cross-bedded units, charcoal is concentrated in foreset cross-beds (Fig. S4a). In sample AC003, we have noted abundant charcoal, often up to 5 mm in size. Secondary wood charcoal from Arlington Canyon samples tends to dominate (Table 1). However, there is an equal proportion of conifer (Fig. 4a–c) and angiosperm

(Fig. 4f–i) wood charcoal throughout the sequence (Fig. 4). In addition, small herbaceous angiosperm axes (Fig. 4j) are common in some samples, but leaf (Fig. 4d,e), bark charcoal and seeds are relatively rare.

Carbonaceous spherules and 'elongate' forms

Firestone *et al.* (2007) coined the term 'carbon spherules', referring to 'highly vesicular, subspherical-to-spherical objects

Table 1. Distribution of charcoal and other organic materials from site III, Arlington Canyon.

Sample No.	Section	Height above base (cm)	Charcoal					Mixed uncharred and charred			Uncharred	
			>1 cm	5 mm–1 cm	<5 mm	<1 mm	1–2 mm axes	leaves	Spherules	Coprolites	Glassy carbon	Wood
SRI-10-47	IIIA	10–12		C		C	R	P		C		
SRI-10-48	IIIA	20–22			A	C	R	R		C		
SRI-10-49	IIIA	27				R						
SRI-10-50	IIIA	69				R						
SRI-10-51	IIIA	53			C		R		R	R	R	
SRI-10-52	IIIA	62	P				P			A		
SRI-10-53	IIIA	72					P			R	R	
SRI-10-54	IIIA	88	C				R			R		
SRI-10-55	IIIA	95	A				R		R	A	P	
SRI-10-56	IIIA	118–120	A	C	C	F				A		C
SRI-10-57	IIIA	131	C	C	F	F		R		R	C	C
SRI-10-58	IIIA	147–148	A	F	F	F			R	R		C
SRI-10-59	IIIA	197–198				F		R		R		
SRI-10-60	IIIA	260										
SRI-10-61	IIIA	131		F					R			F
SRI-10-62	IIIA	131	R				R			R		
SRI-10-63	IIIA	215	P	A			F	P		C		
SRI-10-65	IIIB	55		A	F	F				F		
SRI-10-66	IIIB	83				R				R		
SRI-10-67	IIIB	110				R				R		
SRI-13-01	IIID	118–120			A	A			R	C		
SRI-13-02	IIID	135–140		A	A			C				
SRI-13-03	IIID	154–156				F		R				
SRI-13-04	IIID	200–202			A		F	R	R	R		
SRI-13-05	IIID	210–212		C	C			C		A	R	
SRI-13-05	IIID	270–242			C					C		
SRI-13-07	IIID	15–17		C			F	P	R	C		
SRI-13-08	IIID	28–30		C			R					
SRI-13-09	IIID	40–42	C				F			C	R	F
SRI-13-10	IIID	60–62		C			F		R	C		
SRI-13-11	IIIF	0–4			A			P		C		F
SRI-13-12	IIIF	50–52	A	F	F			C	R	F		P
SRI-13-13	IIIF	115–117			R							
SRI-13-14	IIIF	125–127			C				R	R		
SRI-13-15	IIIF	150–152		A				C		C	P	
SRI-13-16	IIIF	190–192		A				F	R	C	R	
SRI-13-17	IIIF	200–202			C			C		F		
SRI-13-18	IIIF	220–222				A		R		F	R	
SRI-13-19	IIIF	140–142	A	C								A
SRI-13-20	IIIE	100–102	C	C				C		F		
SRI-13-21	IIIE	153–155		A	A					C	R	
SRI-13-22	IIIE	192–194		P	A			C		F		
SRI-13-23	IIIE	218–220			C			F		F	R	
SRI-13-24	IIIC	12–15	A	A	C				C	C		

A, abundant; C, common; F, frequent; R, rare; P, present.

0.15–2.5 mm in diameter, with cracked and patterned surfaces, a thin rind, and honeycombed (spongy) interiors'. According to Firestone *et al.* (2007), these particles were formed during high-temperature ignition associated with the Younger Dryas extraterrestrial impact event. Kennett *et al.* (2008) identified 'carbon elongates', which were described as similar in size, context, and origin, but ellipsoidal in shape and with 'a much coarser interior cellular structure'. In our Arlington samples, carbonaceous spherular forms occur throughout the section but are more common in the basal 2 m (Table 1) (Fig. 3; Supplementary Material, Fig. S7). They range in size from 250 µm to 1.5 mm in diameter. In cross-section, they

often show a thin surface rind and internally a spongy internal texture (Fig. S7). The internal anatomy of these spherules is very diverse. Most of the spherules are black. Our sediment sample AC003 from West contains common carbonaceous spherules (Fig. S5f).

Carbonaceous particles that match the description of 'carbon elongates' occur throughout Locality III and other Arlington sections and are very abundant within several samples (Fig. S8) (e.g. SRI-10-56; Table 1). Some 'elongate' forms show hexagonal morphology (Fig. S8f). In most samples they are black, but in SRI-10-55 they show a range of colours from brown to black (Fig. S8b). Sample AC003 contains a few 'carbon elongates'.

'Glassy carbon'

Firestone *et al.* (2007) also identified glass-like carbon, consisting of angular fragments up to several centimetres in size, with glassy texture 'suggest[ing] melting during formation' purportedly recording impact-generated, high-intensity fire. Material that could be described as 'glassy carbon' occurs throughout the Arlington section but is rarely abundant (Table 1). It occurs as small pieces usually a few millimetres in size (Fig. 3i). It is common in sample SRI-10-55 from Log IIIa. Sample AC003 from West contains a few specimens of glassy carbon.

Three samples of 'glassy carbon' from Arlington Canyon were examined by analytical pyrolysis/gas chromatography/mass spectrometry and compared with samples of charcoal prepared by treatment of *Sequoia* at 350, 450 and 600 °C (Scott and Glasspool, 2005) and with a sample of synthetic glassy carbon (Alfa-Aesar 42130, Type 1, 200–400 µm, spherical). While we do not believe that there is any similarity between 'glassy carbon' as recorded in sediments and true commercially produced glassy carbon, we nevertheless examined both materials. As anticipated, the synthetic glassy carbon, which is specified to be stable up to 1100 °C, gave no chromatographic peaks. The chromatograms of the *Sequoia* and Santa Rosa samples are shown in Fig. S9f, and compared in a bar chart showing the relative percentage peak areas of the 16 most prominent compounds present (Table 2).

Nanodiamonds

We examined three different specimen sets of carbonaceous spherules for the presence of nanodiamonds: (i) five spherules/fragments from SRI 09-28A; (ii) eight spherules/fragments from AC003; and (iii) 13 acid-washed spherules/fragments from AC003. For a detailed discussion on the interpretation of this evidence please refer to Daulton *et al.* (2016).

Data interpretation

Charcoal

The majority, but not all, of charcoal found in Quaternary terrestrial sediments comes from wildfires (Glasspool and Scott, 2013). Most modern charcoal accumulations within fire areas are produced by the charring of surface litter from low-temperature surface fires (Scott, 2010; Scott *et al.*, 2014). Higher temperature crown fires often completely combust the plant material and leave no macroscopic charcoal residue. Charcoal in fluvial settings may indicate not only fire occurrence but also, in some circumstances, deposition during post-fire erosion (Brown *et al.*, 2013). Charcoal type also may indicate burning of trees, shrubs or herbs (Scott, 2010). In this study, charcoal from Arlington Canyon was derived from conifer trees, angiosperm trees and shrubs, and herbaceous angiosperms. This suggests that the fire was probably predominantly a surface fire (Scott *et al.*, 2000; Scott, 2010).

Carbonaceous spherular forms

Two carbonaceous forms – widely known within palaeobotanical circles, but perhaps less so elsewhere – have been reported in samples from Arlington Canyon and have created much confusion. Carbonaceous spherular forms (so-called 'carbon spherules') ranging in size from <100 µm to over 1 mm occur frequently in charcoal residues from most wildfires. Such material is particularly common in charred litter from surface fires. Even in the case of a hot crown fire,

most charcoal comes from the charring of surface-dwelling plants and litter (Scott, 2010).

One of the most common spherular types found in the Arlington Canyon samples are fungal sclerotia (Fig. S7). Sclerotia are common both in the soil and attached to living and dead plant debris. The sclerotia are resting cysts (Fig. S5) that often form during periods of water stress (Amasya *et al.*, 2015). Their occurrence in charcoal residues is not unexpected. The genus *Sclerotium* is common, but in both modern and Quaternary sediments, *Cennococcum* is also widespread (Ferdinandson and Winge, 1925; Sakagami and Watanabe, 2009; Benedict, 2011). Sclerotia have a distinctive morphology: in cross-section they have a thin crust, and the interior may be foam-like (Fig. S7). Their texture can be modified by fire, and the level of modification is a function of temperature (Scott *et al.*, 2010). Just as with wood and other fungal material, the reflectance of charred sclerotia increases with increasing temperatures (Scott and Glasspool, 2007; Scott, 2010). The number of sclerotia in a sediment sample will be controlled by their abundance in the source area and by sedimentological processes. Many fluvial processes concentrate organic matter, including sclerotia (Malloch *et al.*, 1987).

Carbonaceous spherular forms are found throughout the Arlington sequence but are more common near the base of the section. This concentration may be due to either external factors (greater concentration of the presumed source material) or internal processes such as sedimentary concentration (in the low-energy, fine-grained deposits that predominate near the base of the Arlington sequence). It is possible that carbonaceous spherular forms have multiple origins, but most 'carbon spherules' that we have examined can be confidently identified as fungal sclerotia (see also discussion in Daulton *et al.*, 2016).

'Carbonaceous elongates'/coprolites

The elongate forms described by Kennett *et al.* (2008) also may have a range of origins. Some may represent fungal sclerotia (Sakagami and Watanabe, 2009). However, by far the most common origin is arthropod faecal pellets (coprolites) (Scott, 1992). Arthropod coprolites are abundant in fluvial and indeed all terrestrial sediments since the Devonian (e.g. Scott, 1977; Chaloner *et al.*, 1991; Scott, 1992; Habgood *et al.*, 2003; Edwards *et al.*, 2012). They may be produced by a wide range of arthropods, the smallest (<50 µm) from mites, to collembola and termites, and the largest coprolites (>1 mm) from millepedes (Scott, 1992). These particles have a range of shapes and contents. Many of the coprolites from the sediments at Locality III in Arlington are cylindrical with rounded ends (Fig. S8). These are uncharred, partially charred or occur as charcoal (Fig. S8b). When charred, coprolites may shrink and the inside preferentially combust, leaving hollow shells. A significant number of the Arlington coprolites have a hexagonal cross-section, which is typical of termite frass (Light, 1930; Lance, 1946; Scott, 1992; Collinson, 1999; Colin *et al.*, 2011) (Fig. S8d). Such frass is abundant in archaeological deposits (Adams, 1984) and has been identified at other California sites (Light, 1930; Lance, 1946; Anderson and Stillick, 2013). We have experimentally charred termite frass at a range of temperatures. We found that the outer shape is retained and the reflectance increases with temperature (McParland *et al.*, 2007; Scott and Glasspool, 2007).

Glassy carbon

Some carbonaceous materials found in sediments have been termed 'glassy carbon' because they exhibited a glassiness

Table 2. List of compounds detected by pyrolysis-gas chromatography-mass spectrometry of glassy carbon and charcoals.

Ret Time	compound	SEQ350		SEQ450		SEQ600		AC003		SRI-10-36		SRI-10-57	
		Peak Area	%										
1	benzene	3870640	10.77	7580848	14.58	40095737	63.33	3269558	13.64	5264142	49.05	10828341	47.92
2	toluene	7961682	22.15	11875708	22.84	9754648	15.41	6938243	28.95	1952563	18.19	3464002	15.33
3	ethylbenzene	221024	0.61	466479	0.90	1496316	2.36	601975	2.51	190718	1.78	0	0.00
4	xylene	1531400	4.26	2302114	4.43	704280	1.11	1350791	5.64	291081	2.71	93810	0.42
5	styrene	975975	2.72	1184472	2.28	4603983	7.27	1218587	5.09	390031	3.63	324752	1.44
6	phenol	9613598	26.74	8787116	16.90	0	0.00	2488814	10.39	430317	4.01	497775	2.20
7	benzotrile	0	0.00	101814	0.20	0	0.00	954222	3.98	0	0.00	646202	2.86
8	benzofuran	1187128	3.30	1338316	2.57	0	0.00	991371	4.14	0	0.00	0	0.00
9	2-methylphenol	2085471	5.80	1878744	3.61	0	0.00	1838438	7.67	0	0.00	0	0.00
10	4-methylphenol	4177201	11.62	3869322	7.44	0	0.00	2038107	8.50	0	0.00	0	0.00
11	naphthalene	1902648	5.29	4387767	8.44	5362078	8.47	848406	3.54	1386444	12.92	3971877	17.58
12	methylnaphthalene	820391	2.28	1924983	3.70	334955	0.53	478329	2.00	114184	1.06	320448	1.42
13	methylnaphthalene	300671	0.84	815107	1.57	286347	0.45	349751	1.46	99494	0.93	172470	0.76
14	acenaphthene	0	0.00	438952	0.84	0	0.00	178534	0.75	248839	2.32	718862	3.18
15	dibenzofuran	849154	2.36	1381920	2.66	276435	0.44	262903	1.10	70450	0.66	435839	1.93
16	phenanthrene	355260	0.99	921184	1.77	399201	0.63	113065	0.47	256888	2.39	1124154	4.97
17	anthracene	94274	0.26	2747425	5.28	0	0.00	42551	0.18	36582	0.34	0	0.00
	Peak Area Totals	35946517		52002271		63313980		23963645		10731733		22598532	

'Ret Time' is chromatographic retention time (min) and reflects the size and polarity of molecules arriving at the mass spectrometer.

or vitreous appearance (Scheel-Ybert, 1998). Material of the same name – but structurally and chemically distinct – was also synthesized by carbonization of polymer precursors starting in the mid-1950s. True glassy or vitreous morphology in carbonaceous materials does not result exclusively from high temperatures (Fabre, 1996; Marguerie and Hunot, 2007), but can also result from the fine-grained homogenous nature of the material. McParland *et al.* (2010) showed that neither the charcoals associated with glassy carbon, nor the glassy carbon itself in the sediments exhibited features of high-temperature formation. Another explanation for the origin of glassy carbon comes from the charcoalification process itself, which involves pyrolysis in the absence of oxygen (Beaumont, 1985, section 2.5; Scott, 2010).

The chromatogram of the pyrolysate of sample AC003 (Fig. S9d) shows a composition similar to those obtained from samples of *Sequoia* experimentally charred at 350 °C and 450 °C (Fig. S9bc). In addition to aromatic hydrocarbons, oxygen- and nitrogen-containing compounds, namely pyridine, phenol, benzonitrile, benzofuran, methylphenols and dibenzofuran, are present. The chromatograms of the 350 °C and 450 °C experimental *Sequoia* samples and AC003 are similar to those obtained by Kaal *et al.* (2009) from 6200-year-old Fabaceae-derived charcoal from Campo Lamiero, north-west Spain. The implication is that the charcoal sample AC0003 was formed at a temperature <600 °C. Chromatograms produced from samples 10-36 and 10-57 (Fig. S9e,f) resemble those of the 600 °C *Sequoia* charcoal (Table 2). The implication is that these charcoals were formed at a higher temperature than that experienced by sample AC003, but there is no evidence from this analysis of their formation at >1000 °C.

Based on the chromatographic and combustion results from the Arlington Canyon samples, we conclude that much of this glassy carbon was probably produced as solidified tar. Tar is produced during charcoalification, mostly at temperatures below 500 °C (Beaumont, 1985), and this represents the typical temperatures of many surface fires (Scott *et al.*, 2014). The chemistry of tars produced during this process is well understood (e.g. Ku and Mun, 2006).

What we can and cannot say about charcoal in fluvial sediments at Arlington Canyon.

Quantity of charcoal

The quantity of charcoal in any one sample from fluvial sediments is not indicative of the size of a fire. The amount of charcoal depends on the amount of charred litter, as most macroscopic charcoal comes from the charring of surface-dwelling plants and litter from low-temperature surface fires (Scott, 2010). In addition, charcoal can be locally concentrated in some facies (Glasspool and Scott, 2013). After the Hayman fire in Colorado in 2002, charcoal was transported out of the fire-affected area by flooding rivers. One downstream channel was filled with several metres of charcoal (see fig. 9c of Scott, 2010), which was not indicative of the size of the fire but rather of taphonomic processes.

Local or regional fire

Large charcoal fragments may be transported a considerable distance. Large pieces (>1 cm) of charcoal may be transported down rivers and into marine sediments (e.g. Nichols *et al.*, 2000; Scott, 2010). Un-charred and charred plants have different hydrodynamic qualities, as do different plant organs and charcoal formed at different temperatures (e.g. Nichols *et al.*, 2000; Scott, 2010; Scott *et al.*, 2014). It is

reasonable to infer that a fire was local if there is charcoal from a variety of plants, of a range of sizes and varying from charred to un-charred.

Intensity, severity or type of fire

There has been much confusion of the terms 'fire intensity', 'fire severity' and 'burn severity' (Keeley, 2009). Fire intensity refers to the total energy released by a fire and not the energy release rate. Fire intensity data do not provide information on the temperature of the fires or surface fire conditions. It is not possible to determine fire intensity simply from the amount of charcoal. Fire severity refers to the extent of loss or damage to vegetation, which again cannot be determined from charcoal assemblages. It is possible to obtain some temperature data from the measurement of the reflectance of charcoal (Scott, 2010), and charcoal temperature profiles may help to distinguish the occurrence of ground, surface or crown fires (McParland *et al.*, 2009; Hudspith *et al.*, 2014; Scott *et al.*, 2014). Ground fires, as opposed to surface fires, tend to destroy the vegetation, with little charcoal remaining. Crown fires can reach higher temperatures than most surface fires.

Vegetation affected by wildfire

An important feature of charcoal is that it retains anatomical information that allows taxonomic identification (Scott, 2010). The charcoal from the Arlington section is mainly from coniferous and angiosperm secondary wood and indicates that a forested ecosystem was affected by wildfire. However, small axes of herbaceous angiosperms and shrubs suggest that fire on this landscape included mainly surface fire. The reduction of charcoal at higher levels in the Arlington sequence probably results from the documented loss of most large conifers from the Northern Channel Islands by the end of the Pleistocene (Anderson *et al.*, 2010). Grasslands produce much smaller inputs of charcoal (Bond, 2015).

What can and cannot be interpreted from organic fractions

The occurrence of fungal sclerotia tells us little about the environment of deposition, and less about fire regime. They are common in many soils and especially those of temperate and arctic–alpine climatic zones (Sakagami and Watanabe, 2009). However, more sclerotia are formed during periods of water stress, so there may be some indication of rainfall variability (Benedict, 2011; Fernandez and Koide, 2013). The sizes of coprolites that are composed of plant material

may also indicate the occurrence of mites, springtails and millipedes, all found in decaying plant litter (e.g. Chaloner *et al.*, 1991; Scott, 1992), or of termites, which tend to be found in somewhat drier environments (Harris, 1971).

Dating

Eleven radiocarbon dates were obtained from site III primarily from charcoal fragments and also from a piece of uncharred wood (Table 3). All new dates are shown calibrated using the IntCal13 calibration curve (Reimer *et al.*, 2013) using OxCal v4.2.4 (Bronk Ramsey and Lee, 2013) (Table 3). The oldest age returned was 14080–14500 cal a BP, and the youngest age 12710–12850 cal a BP (Fig. S2c). These new chronological data are consistent with the radiocarbon dates presented in Kennett *et al.* (2008) from the same locality. However radiocarbon dates on charcoal fragments from elsewhere in Arlington Canyon and from similar deposits in neighbouring canyons shows deposition and fire activity as early as 29222–28394 cal a BP (Pinter *et al.*, 2011), with charcoal diminishing in quantity higher in the Arlington sequence, but on-going into the Holocene (Anderson *et al.*, 2010). Indeed, the distribution of charcoal through Arlington Canyon clearly indicates a record of more than one fire event, as shown in both the wider chronological and sedimentological evidence (Hardiman *et al.*, 2016). These data are inconsistent with the single, catastrophic impact-induced ignition interpreted by Firestone *et al.* (2007), Kennett *et al.* (2008) and other YDIH proponents.

Discussion

Like many Quaternary deposits, the fluvial sequence in Arlington Canyon contains a significant quantity and range of organic material, much of which has been charred. Abundant charcoal implies the occurrence of fire, but whether these fires were started by lightning, humans or extraterrestrial impact requires additional lines of evidence (Hardiman *et al.*, 2016; Scott *et al.*, 2016).

Arlington Canyon has featured centrally in results suggesting a global-scale impact drove broad changes at the onset of the Younger Dryas (the YDIH). Wittke *et al.* (2013) assert that we did not study the same section as theirs (AC003). This is not true. While Kennett *et al.* (2008, 2009b) gave UTM coordinates without specifying which datum or map projection was used, we were able to navigate to their published location using the North American Datum 1983 (NAD83) and found there the largest, best exposed, and most accessible outcrop in Arlington Canyon. Later we surmised that

Table 3. New radiocarbon dates obtained from Site III, Arlington Canyon, Santa Rosa Island, in this study.

¹⁴ C publication code	Site signifier	Sample no.	Dated material	δ ¹³ C (‰)	¹⁴ C age (a BP)	¹⁴ C age error (1σ)	Reference*
UCIAMS-84951	IIIa	SRI-10-63	Charcoal	–	11 005	25	1
UCIAMS-84950	IIIa	SRI-10-63	Charred coprolites	–	11 755	30	1
UCIAMS-84949	IIIa	SRI-10-62	Charred twigs	–	11 030	30	1
UCIAMS-84948	IIIa	SRI-10-61	Uncharred wood	–	10 935	30	This study
UCIAMS-84947	IIIa	SRI-10-56	Charred coprolites	–	11 095	30	1
UCIAMS-84946	IIIa	SRI-10-56	Charred twigs	–	11 035	30	1
UCIAMS-84945	IIIa	SRI-10-52	Charred twigs	–	11 000	25	1
UCIAMS-84944	IIIa	SRI-10-47	Charred twigs	–	12 310	30	1
UCIAMS-84943	IIIa	SRI-10-47	Charred coprolites	–	11 885	30	1
OxA-29224	IIIf	SRI-13-11	Small charred axis	–24.55	11 130	50	1
OxA-29225	IIIf	SRI-13-11	Small charred axis	–24.62	11 085	50	1

*1, Hardiman *et al.* (2016).

Kennett *et al.* (2008, 2009b) had used NAD27 (confirmed in Wittke *et al.*, 2013). We subsequently measured, sampled, and dated the small section at that location.

We have described, analysed and sampled sequences in Arlington and in other canyons on Santa Rosa Island, which include material ranging in age from ~29 000 cal a BP to ~5000 a BP (Scott, 2010; Pinter *et al.*, 2011; Hardiman *et al.*, 2016). We continue to be puzzled why YDIH proponents have focused extraordinary attention on one single age horizon in one <5-m section, when such a broad range of deposits and ages are represented in the surrounding area (see Hardiman *et al.*, 2016). We show from our lithological logging and analysis that there was not an 'impact horizon' as claimed.

Carbonaceous materials from Arlington Canyon do not require extraterrestrial input or ignition, or in some cases preclude such an event. Carbonaceous spherular forms ('carbon spherules') and coprolites ('carbon elongates') occur in multiple samples from multiple horizons on Santa Rosa Island and on neighboring islands and from sites throughout the world. They occur in sediments of a wide range of ages, from well before the Younger Dryas to well after (e.g. Anderson *et al.*, 2010; Scott, 2010) (Table 1). Many of the carbonaceous spherular forms have features identical to those of fungal sclerotia. None of the samples or morphologies observed to date require catastrophic high-temperature combustion or other extraterrestrial influence. Many of the 'carbon elongates' are demonstrated to be arthropod faecal pellets (Fig. S8); those with hexagonal morphology are identified as termite frass (see Scott, 1992).

Many YDIH proponents repeatedly use glassy carbon as an indicator of high-temperature fires (Firestone *et al.*, 2007; Kennett *et al.*, 2008; Bunch *et al.*, 2012; Wittke *et al.*, 2013; Kinzie *et al.*, 2014). Most glassy carbon is in fact produced as solidified tars from a low- to medium-temperature charring process, as shown here, being common in fires of those temperatures. This has also been referred to as vitreous charcoal, glassy charcoal, etc., by numerous authors and was demonstrated by McParland *et al.* (2010) to be of low-temperature origin. None of the carbon forms from Arlington Canyon yield evidence of higher-than-normal burning temperatures.

Wood charcoal is abundant in lower portions of the Arlington Canyon sequence, including from deposits both older and younger than the Younger Dryas. Charcoal distribution in fluvial sediments is strongly influenced by taphonomic processes, so the type and quantity of charcoal varies both laterally and vertically. The number of charcoal particles per unit volume or weight of sediment samples cannot be interpreted in terms of 'fire frequency' or 'fire intensity'.

Kennett *et al.* (2008, 2009b) repeat the narrative from Firestone *et al.* (2007) that the purported Younger Dryas impact created intense wildfires across much of the planet, including in particular, Santa Rosa Island. Marlon *et al.* (2009) found no evidence of regionally synchronous fires across North America, and the current study finds no evidence of high-temperature fires in Arlington Canyon. The occurrence of 'carbon spherules' does not indicate high temperature. Spherules and charcoal from AC003 had low reflectance, typical of low-temperature surface fires. Wittke *et al.* (2013) claim to have produced spheres from high-temperature experiments involving combusting wood (their fig. 8). However, these are not carbon spheres but rather are inorganic in composition, comprising aluminium and silica and are not relevant to the origin of the carbonaceous spherules.

The occurrence of nanodiamonds, particularly the hexagonal 2H polytype lonsdaleite, in Younger Dryas boundary

sediments is considered by YDIH proponents as among the strongest evidence of impact shock processing of the crust. We have demonstrated elsewhere (Daulton *et al.*, 2016) that the observations and interpretations were erroneous.

We conclude that YDIH proponents fail to explain the broad discrepancies between their interpretations and the findings of independent researchers. Contrary evidence is ignored, and a broad range of terrestrial evidence is interpreted through the lens of a presumed extraterrestrial impact. On Santa Rosa Island (Pinter *et al.*, 2011) as well as other California Channel Islands (Pigati *et al.*, 2014), widespread and frequent fires occurred both before and after the onset of the Younger Dryas, recording predominantly low-temperature surface fires. Stratigraphic concentrations of charcoal are related to the nature of the original fires but also to how much litter there was to char and a wide range of other taphonomic as well as transportation and depositional processes. The sediments in Arlington Canyon lack evidence for meteoritic/cometary material from an impact in North America, evidence of associated impact processes and evidence of impact-generated fires (see also comments by Boslough *et al.*, 2013).

Conclusions

Fluvial deposits in Arlington Canyon, Santa Rosa Island, and material in those deposits document a long-term and mostly gradual evolution of the Arlington palaeo-landscape since the latest Pleistocene. This was driven by some combination of climate change, post-glacial sea-level rise, climate-driven vegetation changes, extinction of the local megafauna (*Mammuthus exilis*), and the arrival and subsequent expansion of human activities (e.g. Rick *et al.*, 2014). These changes have driven a long-term shift in fire regimes. The size range of the charcoal fragments in the latest Pleistocene to Holocene sediments from Arlington Canyon, as well as the presence of charred and non-charred plant material, suggests a surface fire regime, with charcoal moved to the stream by overland flow and subsequent fluvial transport. This range of material, together with scanning electron microscopy and reflectance analyses, indicates low-temperature surface-fire regimes of coniferous and mixed coniferous/angiosperm forests. The distribution of charcoal in the sequence suggests multiple fire events through the record. We find no evidence for a single, high-intensity crown fire, nor any evidence of the kind of catastrophic, transformative fire event proposed in the YDIH.

Carbonaceous spherules recorded by Kennett *et al.* (2008) are predominantly fungal sclerotia, and 'carbon elongates' are predominantly arthropod coprolites; those with hexagonal cross-sections probably are termite frass. Glassy carbon present in these deposits formed from the precipitation of tars during the charcoalification process. None of these materials indicate high temperatures. The presence of nanodiamonds in Arlington Canyon spherules has not been confirmed by independent studies, and we find no evidence of nanodiamonds. Material identified as lonsdaleite at Arlington Canyon by Kennett *et al.* (2009b) is inconsistent with the lonsdaleite structure and more consistent with polycrystalline aggregates of graphene and graphane (see Daulton *et al.*, 2010, 2016). None of the evidence supports the contention that there is an impact horizon in the Arlington sequence. By extension, our research suggests that similar problems may exist at other sites supporting the purported Younger Dryas impact.

Supplementary Material

- Fig. S1.** Photograph of outcrop of Site III, Arlington Canyon.
Fig. S2. The central part of the Site III section (AC003) of Kennett *et al.* (2008, 2009b) and Wittke *et al.* (2013) at Arlington Canyon.
Fig. S3. Lateral variation of facies at the base of the section at Site III, Arlington Canyon.
Fig. S4. Sediments and carbonaceous fossils from our locality III in Arlington Canyon, which is the same locality as AC003 of Kennett *et al.* (2008, 2009b) and Wittke *et al.* (2013).
Fig. S5. Sieved samples (>125 µm) from Site III Arlington Canyon.
Fig. S6. Sediments and charcoal from Site III, Arlington Canyon.
Fig. S7. Carbonaceous spherules from Arlington Canyon, Site III.
Fig. S8. Coprolites ('carbon elongates') from Arlington Canyon, Site III.
Fig. S9. Chromatograms of charcoals pyrolysed at 650 °C.

Acknowledgements. We thank staff with Channel Islands National Park. ACS thanks Sharon Gibbons and Neil Holloway for technical support. We also thank Tom Higham of the Oxford Accelerator Unit for dates and for his comments on the manuscript. This research was supported by grants from the National Geographic Society (8321-07) to NP, from the National Science Foundation (EAR-0746015) to NP and RSA, and a Leverhulme Emeritus Fellowship (EM-2012-054) to ACS.

References

- Adams KR. 1984. Evidence of wood-dwelling termites in archaeological sites in the southwestern United States. *Journal of Ethnobiology* **4**: 29–43.
- Amasya AF, Narisawa K, Watanabe M. 2015. Analysis of sclerotia-associated fungal communities in cool-temperate forest soils in North Japan. *Microbes and Environments* **30**: 113–116.
- Anderson RS, Starratt S, Jass RMB *et al.* 2010. Fire and vegetation history on Santa Rosa Island, Channel Islands, and long-term environmental change in southern California. *Journal of Quaternary Science* **25**: 782–797.
- Anderson RS, Stillick RD. 2013. 800 years of vegetation change, fire and human settlement in the Sierra Nevada of California, USA. *The Holocene* **23**: 823–832.
- Beaumont E (ed.). 1985. Industrial charcoal making. *FAO Forestry Paper* **63**. Food and Agricultural Organization of the United Nations: Rome (<http://www.fao.org/docrep/X5555E/x5555e00.htm#Contents>).
- Benedict JB. 2011. Sclerotia as indicators of mid-Holocene tree-limit altitude, Colorado Front Range, USA. *The Holocene* **21**: 1021–1023.
- Bird MI. 2013. Charcoal. In *Encyclopaedia of Quaternary Science*, Elias Scott A, and Mock Cary J, (eds). Elsevier Science: Amsterdam, The Netherlands; 353–360.
- Bond WJ. 2015. Fires in the Cenozoic: a late flowering of flammable ecosystems. *Frontiers in Plant Science* **5**: 749.
- Boslough M, Harris AW, Chapman C *et al.* 2013. Younger Dryas impact model confuses comet facts, defies airburst physics. *Proceedings of the National Academy of Sciences USA* **110**: E4170.
- Bridgland DR, Westaway R. 2014. Quaternary fluvial archives and landscape evolution: a global synthesis. *Proceedings of the Geologists' Association* **125**: 600–629.
- Bronk Ramsey C, Lee S. 2013. Recent and planned developments of the program OxCal. *Radiocarbon* **55**: 720–730.
- Brown SAE, Collinson ME, Scott AC. 2013. Did fire play a role in formation of dinosaur-rich deposits? An example from the Late Cretaceous of Canada. *Palaeobiodiversity and Palaeoenvironments* **93**: 317–326. Doi: 10.1007/s12549-013-123-y.
- Bunch TE, Hermes RE, Moore AMT *et al.* 2012. Very high-temperature impact melt products as evidence for cosmic airbursts and impacts 12,900 years ago. *Proceedings of the National Academy of Sciences USA* **109**: E1903–E1912.
- Chaloner WG, Scott AC, Stephenson J. 1991. Fossil evidence for plant-arthropod interactions in the Palaeozoic and Mesozoic. *Philosophical Transactions of the Royal Society of London* **B333**: 177–186.
- Colin J, Néraudeau D, Nel A *et al.* 2011. Termite coprolites (Insecta: Isoptera) from the Cretaceous of western France: a palaeoecological insight. *Revue de Micropaléontologie* **54**: 129–139.
- Collinson ME. 1999. Plants and animal diets. In *Fossil plants and spores*, Jones P, Rowe NP. (eds). Geological Society: London; 316–320.
- Daulton TL, Amari S, Scott AC *et al.* 2016. Comprehensive analysis of nanodiamond evidence relating to the Younger Dryas Impact Hypothesis. *Quaternary Journal of Science* **32**: 7–34.
- Daulton TL, Pinter N, Scott AC. 2010. No evidence of nanodiamonds in Younger-Dryas sediments to support an impact event. *Proceedings of the National Academy of Sciences USA* **107**: 16043–16047.
- Edwards D, Selden PA, Axe L. 2012. Selective feeding in an Early Devonian terrestrial ecosystem. *Palaios* **27**: 509–522.
- Fabre L. 1996. *Le charbonnage historique de la chênaie à Quercus ilex L. (Languedoc, France): conséquences écologiques*. Thèse de Doctorat. USTL: Montpellier.
- Ferdinandson C, Winge Ö. 1925. *Cenococcum Fr.: a monographic study*. Den Kongelige Veterinaer-og Landbohøjskole Aarskrift; 332–382 (in Danish).
- Fernandez CW, Koide RT. 2013. The function of melanin in the ectomycorrhizal fungus *Cenococcum geophilum* under water stress. *Fungal Ecology* **6**: 479–486.
- Firestone RB, West A, Kennett JP *et al.* 2007. Evidence for an extraterrestrial impact 12,900 years ago that contributed to the megafaunal extinctions and the Younger Dryas cooling. *Proceedings of the National Academy of Sciences USA* **104**: 16016–16021.
- Gavin DG. 2001. Estimation of inbuilt age in radiocarbon ages of soil charcoal for fire history studies. *Radiocarbon* **43**: 27–44.
- Glasspool IJ, Scott AC. 2013. Identifying past fire events. In *Fire Phenomena in the Earth System – an Interdisciplinary Approach to Fire Science*, Belcher CM (ed.). John Wiley and Sons: Chichester; 179–206.
- Habgood KS, Hass H, Kerp H. 2003. Evidence for an early terrestrial food web: coprolites from the Early Devonian Rhyne chert. *Transactions of the Royal Society of Edinburgh Earth Sciences* **94**: 371–389.
- Hardiman M, Scott AC, Pinter N *et al.* 2016. Fire history on the California Channel Islands spanning human arrival in the Americas. *Philosophical Transactions of the Royal Society of London. Series B, Biological Sciences* **371**: 20150167.
- Harris WV. 1971. *Termites: Their Recognition and Control*. Longman: London.
- Hendy IL, Kennett JP, Roark EB *et al.* 2002. Apparent synchronicity of submillennial scale climate events between Greenland and Santa Barbara Basin, California from 30–10 ka. *Quaternary Science Reviews* **21**: 1167–1184.
- Holliday VT, Surovell T, Meltzer DJ *et al.* 2014. The Younger Dryas impact hypothesis: a cosmic catastrophe. *Journal of Quaternary Science* **29**: 515–530.
- Hudspith VA, Belcher CM, Yearsley JM. 2014. Charring temperatures are driven by the fuel types burned in a peatland wildfire. *Frontiers in Plant Science* **5**: 714.
- Kaal J, Martínez Cortizas A, Nierop KGJ. 2009. Characterisation of aged charcoal using a coil probe pyrolysis-GC/MS method optimised for black carbon. *Journal of Analytical and Applied Pyrolysis* **85**: 408–416.
- Keeley JE. 2009. Fire intensity, fire severity and burn severity: a brief review and suggested usage. *International Journal of Wildland Fire* **18**: 116–126.
- Kennett DJ, Kennett JP, West GJ *et al.* 2008. Wildfire and abrupt ecosystem disruption on California's Northern Channel Islands at the Allerød–Younger Dryas boundary (13.0–12.9 ka). *Quaternary Science Reviews* **27**: 2530–2545.
- Kennett DJ, Kennett JP, West A *et al.* 2009a. Nanodiamonds in the Younger Dryas boundary sediment layer. *Science* **323**: 94.
- Kennett JP, Kennett DJ, Culleton BJ *et al.* 2015. Bayesian chronological analyses consistent with synchronous age of 12,835–12,735

- Cal B.P. for Younger Dryas boundary on four continents. *Proceedings of the National Academy of Sciences USA* **112**: E4344–E4353.
- Kennett DJ, Kennett JP, West A *et al.* 2009b. Shock-synthesized hexagonal diamonds in Younger Dryas boundary sediments. *Proceedings of the National Academy of Sciences USA* **106**: 12623–12638.
- Kinzie CR, Que Hee SS, Stich A *et al.* 2014. Nanodiamond-rich layer across three continents consistent with major cosmic impact at 12,800 cal BP. *Journal of Geology* **122**: 475–505.
- Ku CS, Mun SP. 2006. Characterization of pyrolysis tar derived from lignocellulosic biomass. *Journal of Industrial and Engineering Chemistry* **12**: 853–861.
- Lance JF. 1946. Fossil arthropods of California. 9. Evidence of termites in the Pleistocene asphalt of Carpenteria, California. *Southern California Academy of Sciences Bulletin* **45**: 21–27.
- LeCompte MA, Goodyear AC, Demitroff MN *et al.* 2012. Independent evaluation of conflicting microspherule results from different investigations of the Younger Dryas impact hypothesis. *Proceedings of the National Academy of Sciences USA* **109**: E2960–E2969.
- Light SE. 1930. Fossil termite pellets from the Seminole Pleistocene. *University of California Publications of the Department of Geological Sciences* **19**: 75–80.
- Malloch D, Grenville D, Hubart J-M. 1987. An unusual subterranean occurrence of fossil fungal sclerotia. *Canadian Journal of Botany* **65**: 1281–1283.
- Marguerie D, Hunot J-Y. 2007. Charcoal analysis and dendrology: data from archaeological sites in north-western France. *Journal of Archaeological Science* **34**: 1417–1433.
- Marlon JR, Bartlein PJ, Walsh MK *et al.* 2009. Wildfire responses to abrupt climate change in North America. *Proceedings of the National Academy of Sciences USA* **106**: 2519–2524.
- McParland LC, Collinson ME, Scott AC *et al.* 2007. Ferns and fires: experimental charring of ferns compared to wood and implications for paleobiology, paleoecology, coal petrology, and isotope geochemistry. *Palaeos* **22**: 528–538.
- McParland LC, Collinson ME, Scott AC *et al.* 2009. The use of reflectance values for the interpretation of natural and anthropogenic charcoal assemblages. *Archaeological and Anthropological Sciences* **1**: 249–261.
- McParland LC, Collinson ME, Scott AC *et al.* 2010. Is vitrification in charcoal a result of high temperature burning of wood? *Journal of Archaeological Science* **37**: 2679–2687.
- Meltzer DJ, Holliday VT, Cannon MD *et al.* 2014. Chronological evidence fails to support claim of an isochronous widespread layer of cosmic impact indicators dated to 12,800 years ago. *Proceedings of the National Academy of Sciences USA* **111**: E2162–E2171.
- Mishra S, White MJ, Beaumont P *et al.* 2007. Fluvial deposits as an archive of early human activity. *Quaternary Science Reviews* **26**: 2996–3016.
- Nichols GJ, Cripps JA, Collinson ME *et al.* 2000. Experiments in waterlogging and sedimentology of charcoal: results and implications. *Palaeoecology Palaeoclimatology Palaeoecology* **164**: 43–56.
- Petaev MI, Huang S, Jacobsen SB *et al.* 2013. Large Pt anomaly in the Greenland ice core points to a cataclysm at the onset of Younger Dryas. *Proceedings of the National Academy of Sciences USA* **110**: 12917–12920.
- Pigati JS, McGeehin JP, Skipp GL *et al.* 2014. Evidence of repeated wildfires prior to human occupation on San Nicolas Island, California. *Monographs of the Western North American Naturalist* **7**: 35–47.
- Pinter N, Ishman SE. 2008. Impacts, mega-tsunami, and other extraordinary claims. *GSA Today* **18**: 37–38.
- Pinter N, Johns B, Little B *et al.* 2001. Fault-related folding in California's Northern Channel Islands documented by rapid-static GPS positioning. *GSA Today* **11**: 4–9.
- Pinter N, Keller EA. 1995. Geomorphological analysis of neotectonic deformation, northern Owens Valley, California. *Geologische Rundschau* **84**: 200–212.
- Pinter N, Scott AC, Daulton TL *et al.* 2011. The Younger Dryas impact hypothesis: a requiem. *Earth Science Reviews* **106**: 247–264.
- Rasmussen SO, Andersen KK, Svensson AM *et al.* 2006. A new Greenland ice core chronology for the last glacial termination. *Journal of Geophysical Research* **111**: D6102.
- Reimer PJ, Bard E, Bayliss A. 2013. IntCal13 and Marine13 radiocarbon age calibration curves 0–50,000 years cal BP. *Radiocarbon* **55**: 1869–1887.
- Rhodes AN. 1998. A method for the preparation and quantification of microscopic charcoal from terrestrial and lacustrine sediment cores. *Holocene* **8**: 113–117.
- Rick TC, Sillett TS, Ghalambor CK *et al.* 2014. Ecological change on California's Channel Islands from the Pleistocene to the Anthropocene. *BioScience* **64**: 680–692.
- Sakagami N, Watanabe M. 2009. Contribution of sclerotia of *Cenococcum* species to soil organic carbon in low pH forest soils. *Goldschmidt Conference, Abstracts* **4009**: A1148.
- Scheel-Ybert R. 1998. *Stabilité de l'écosystème sur le littoral sud-est du Bresil à l'Holocène Supérieur (5500–1400 ans BP)*. PhD Thesis, Université de Montpellier II.
- Schiiffer MB. 1986. Radiocarbon dating and the 'old wood' problem: the case of the Hohokam chronology. *Journal of Archaeological Science* **13**: 13–30.
- Schumann RR, Minor SA, Muhs DR *et al.* 2014. Landscapes of Santa Rosa Island, Channel Islands National Park, California. *Monographs of the Western North American Naturalist* **7**: 48–67.
- Schumann RR, Pigati JS, McGeehin JP. 2016. Fluvial system response to Late Pleistocene–Holocene sea-level change on Santa Rosa Island, Channel Islands National Park, California. *Geomorphology* **268**: 322–340.
- Scott AC. 1977. Coprolites containing plant material from the Carboniferous of Britain. *Palaentology* **20**: 59–68.
- Scott AC. 1992. Trace fossils of plant–arthropod interactions. In *Trace Fossils. Short courses in Paleontology*, 5, Maples CG, West RR (eds). Paleontological Society: Tulsa, OK; 197–223.
- Scott AC. 2010. Charcoal recognition, taphonomy and uses in palaeoenvironmental analysis. *Palaeoecology, Palaeoclimatology, Palaeoecology* **291**: 11–39.
- Scott AC, Bowman DJMS, Bond WJ *et al.* 2014. *Fire on Earth: an Introduction*. John Wiley and Sons: Chichester.
- Scott AC, Chaloner WG, Belcher CM *et al.* 2016. The interaction of fire and mankind: introduction. *Philosophical Transactions of the Royal Society of London. Series B, Biological Sciences* **371**: 20150162.
- Scott AC, Cripps JA, Collinson ME *et al.* 2000. The taphonomy of charcoal following a recent heathland fire and some implications for the interpretation of fossil charcoal deposits. *Palaeoecology Palaeoclimatology Palaeoecology* **164**: 1–31.
- Scott AC, Glasspool IJ. 2005. Charcoal reflectance as a proxy for the emplacement temperature of pyroclastic flow deposits. *Geology* **33**: 589–592.
- Scott AC, Glasspool IJ. 2007. Observations and experiments on the origin and formation of inertinite group macerals. *International Journal of Coal Geology* **70**: 53–66.
- Scott AC, Pinter N, Collinson ME *et al.* 2010. Fungus, not comet or catastrophe, accounts for carbonaceous spherules in the Younger Dryas "impact layer". *Geophysical Research Letters* **37**: L14302.
- van Hoesel A, Hoek WZ, Pennock GM *et al.* 2014. The Younger Dryas impact hypothesis: a critical review. *Quaternary Science Reviews* **83**: 95–114.
- Wittke JH, Weaver JC, Bunch TE *et al.* 2013. Evidence for deposition of 10 million tonnes of impact spherules across four continents 12,800 y ago. *Proceedings of the National Academy of Sciences USA* **110**: E2088–E2097.